CrossMark

ORIGINAL RESEARCH

Synthesis of Co(II) and Cr(III) salicylidenic Schiff base complexes derived from thiourea as precursors for nano-sized Co_3O_4 and Cr_2O_3 and their catalytic, antibacterial properties

Leila Kafi-Ahmadi[1] · Leila Shirmohammadzadeh[1]

Abstract This study focuses on the synthesis of Co(II) and Cr(III) Schiff base complexes obtained from thiourea. The complexes were synthesized by template method and characterized by elemental analysis (CHNS), FT-IR, UV–vis spectroscopy, conductivity measurement and magnetic moment. The spectroscopic studies suggested the octahedral and square-pyramidal structures for Co(II) and Cr(III) complexes, respectively. Then the complexes were used as precursors for preparation of Co_3O_4 and Cr_2O_3 nanoparticles via solid-state thermal decomposition without using a catalyst, toxic solvent, template or surfactant and complicated equipment, which makes it efficient, one-step, simple and environment-friendly. The chemical structure of the metal oxides is studied by FT-IR, XRD and SEM. To investigate the applications of the synthesized complexes, in the next step, the complexes were screened for antibacterial activity against clinically important bacteria such as *Escherichia coli*, *Staphylococcus aureus*, and *Bacillus subtilis*. The Cr(III) and Co(II) complexes showed good biological activity against all the tested bacteria. Also, the catalytic activities of the complexes were studied in toluene using non-toxic hydrogen peroxide as the oxidant. The results showed that Co(II) complex has catalytic activity for oxidation of toluene, but Cr(III) complex did not show any catalytic activity.

✉ Leila Kafi-Ahmadi
l.kafiahmadi@urmia.ac.ir

[1] Department of Chemistry, Faculty of Science, Urmia University, Urmia, Iran

Introduction

Schiff bases are synthesized when any primary amine reacts with an aldehyde or a ketone under specific conditions. Structurally, a Schiff base (also known as imine or azomethine) is a nitrogen analogue of an aldehyde or ketone in which the carbonyl group has been replaced by an imine or azomethine group. Schiff base ligands are easily synthesized and form complexes with almost all metal ions. Over the past few years, there have been many reports on their applications in biology including antibacterial [1], antifungal [2], anticancer [3], antioxidant, anti-inflammatory [4], antimalarial [5], antiviral activity [6] and also as catalyst in several reactions such as polymerization reaction, reduction of thionyl chloride, oxidation of organic compounds, reduction reaction of ketones, aldol reaction, Henry reaction, epoxidation of alkenes, hydrosilylation of ketones, Diels–Alder reaction [7, 8]. The central metal ions in these complexes act as active sites for catalyzing chemical reactions such as oxidation of toluene. The controlled oxidation of toluene with H_2O_2 leads to a variety of products such as benzyl alcohol, benzaldehyde and benzoic acid which are industrially very important. H_2O_2 is one of the most straightforward, clean, and versatile oxidants from both an environmental and economic perspective, because H_2O_2 has a high content of active oxygen and its byproduct is water [9].

Recently, several groups used metal complexes as a precursor for preparation of metal oxide nanoparticles by various methods. Considerable efforts have been dedicated to control the shape and size by different methods such as hydrothermal synthesis, microwave, chemical precipitation and the solid-state thermal decomposition methods. Among various techniques for preparation of metal oxide nanoparticles, solid-state thermal decomposition of

transition metal complexes is one of the best method, because it is inexpensive (economical) and does not use toxic solvent (pollution free and surfactant route and is much faster, whereas process conditions, particle size and purity can be easily controlled [10, 11].

In the present paper, we report the synthesis of Co(II) and Cr(III) salicylidenic Schiff base complexes derived from thiourea and studied by elemental analysis (CHNS), FT-IR, UV–vis spectroscopy, conductance measurement and magnetic moment. Then Co_3O_4 and Cr_2O_3 nanoparticles were synthesized from Co(II) and Cr(III) Schiff base complexes by solid-state thermal decomposition method. In the next step, the complexes screened for antibacterial activity against some clinically important bacteria such as *Escherichia coli*, *Staphylococcus aureus*, and *Bacillus subtilis*. Also, the catalytic activities of the complexes were examined in toluene using non-toxic hydrogen peroxide as the oxidant.

Experimental

Materials and methods

All chemicals used were of analytical grade purchased from Merck. The FT-IR analyses were measured with a Fourier transform infrared spectrophotometer (Nexus 670, Thermo Nicolet, USA). The UV–vis spectra were recorded by UV–vis spectrophotometer (T60-PG Instruments Ltd. UK). UV–vis electronic absorption spectrum was measured in diffuse reflectance mode in the 200–800 nm wavelength range. The m.p. of complexes are measured by electrothermal melting point apparatus model BÜCHI 510. The conductometric measurements were carried out with a SELECTA LAB 901 conductometer. CHNS analyses were carried out using an "Elementary Vario EL III" elemental analyzer. The magnetic susceptibility measurements were carried out on vibrating sample magnetometer (Model PAR 155) at room temperature.

Template synthesis of Co (II) (*1*) and Cr(III) (*2*) complexes

Attempt to prepare free ligand was unsuccessful because it is easily hydrolysed in contact with water. Thus the template method was used for the synthesis of complexes.

1 mmol of metal nitrate and 2 mmol of salicylaldehyde were dissolved in 10 mL of ethanol to form homogeneous solutions. Few drops of ammonia solution were added until pH 6–8. Then thiourea solution (1 mmol) was added dropwise to the above solution with stirring. The mixture was allowed to reflux under stirring for 8 h (Scheme 1). After that, the resulting mixture was cooled in room

temperature and filtrated under reduced pressure. The purity of the complex was confirmed by TLC.

The physical properties of complexes are tabulated in Table 1. The results obtained are in good agreement with those calculated for the suggested formula and the melting points are sharp, indicating the purity of the prepared complexes.

Several attempts to obtain a single crystal suitable for X-ray crystallography failed. However, the spectroscopic and magnetic data are able to predict the possible structure of the synthesized complexes.

Synthesis of metal oxides

Metal oxides (Co_3O_4 and Cr_2O_3) were synthesized by the thermal decomposition method [12]. The above complexes was ground to ensure homogeneous powder and then heated at 750 °C for 2 h (Co(II) complex) and 530 °C for 2 h (Cr(III) complex) in a conventional furnace. The obtained precipitate was filtered and washed with ethanol to remove the impurities.

Results and discussion

Conductance measurement and magnetic moment of complexes

Molar conductivity was applied to help in the investigation of the geometrical structures of the complexes. Molar conductance (Λ_M) of 10^{-3} M ethanol solutions of the complexes was determined. The value for Co(II) complex is 159.8 Ω^{-1} cm^2 mol^{-1} consistent with 1:2 electrolyte [13], while the conductivity of the Cr(III) complex is 94.53 Ω^{-1} cm^2 mol^{-1}. Thus this complex behaves as 1:3 electrolyte; consequently, three nitrate ions are present outside the coordination sphere [14].

The Co(II) complex possesses magnetic moment in the range $\mu_{eff} = 4.91$ BM in agreement with octahedral geometry [15, 16]. High-spin octahedral complexes of Co(II) have magnetic moments ranging from 4.7 to 5.2 BM. They have large orbital contribution since the spin-only formula for three unpaired electrons is only 3.88 BM. This value is attributed to threefold orbital degeneracy $^4T_{1g}$ ground state [17]. Magnetic moment of the Cr(III) complex was 4.09 BM at room temperature, which is close to the predicted value for three unpaired electrons in the metal ion [18, 19].

UV–vis spectra of complexes

The electronic spectra of octahedral Co(II) species are theoretically expected to have three spin-allowed
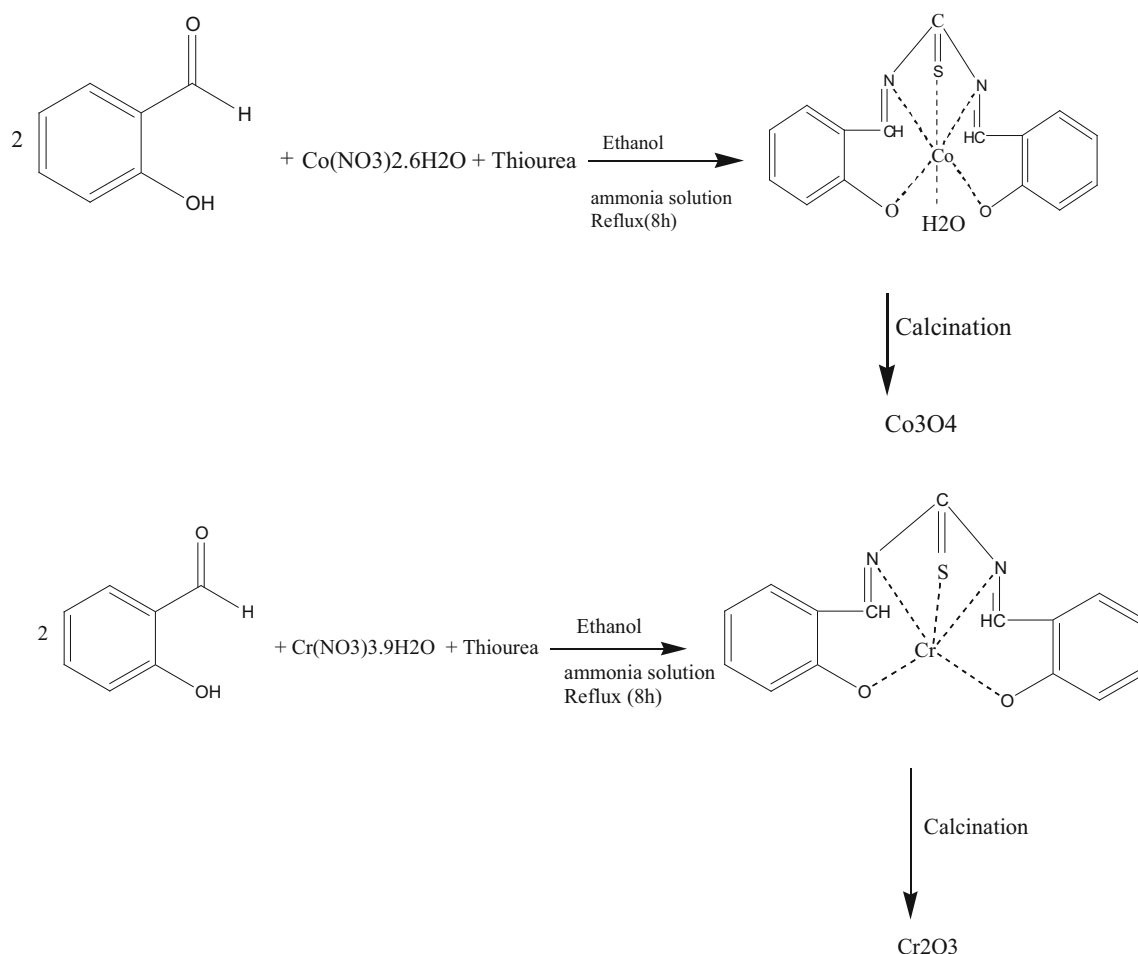
Scheme 1 Template synthesis of Co (II) (*1*) and Cr(III) (*2*) complexes

Table 1 Physical data of the prepared complexes

Yield %	Molecular formula	Color	μ_{eff} (BM)	m.p. (°C)	Λ_M (Ω^{-1} cm^2 mol^{-1})	Elemental analysis found (calcd.)			
						%C	%H	%N	%S
77.1	[C$_{15}$H$_{12}$N$_2$O$_3$SCo]·(NO$_3$)$_2$	Dark brown	4.91	143	159.8	37.41 (37.27)	2.62 (2.48)	11.73 (11.59)	6.95 (6.62)
66.7	[C$_{15}$H$_{10}$N$_2$O$_2$SCr]·(NO$_3$)$_3$·H$_2$O	Dark green	4.09	170	94.53	33.87 (33.45)	2.46 (2.23)	13.38 (13.01)	6.07 (5.94)

transitions from the ground state: $^4T_{1g(F)}$ to $^4T_{2g(F)}$, $^4A_{2g(F)}$ and $^4T_{1g(P)}$, referred to hereafter as υ_1, υ_2 and υ_3, respectively. In addition, spin-forbidden transitions to doublet terms may appear. The second spin-allowed transition, υ_2, in the spectra of oxygen-coordinated octahedral species is usually obscured because of one or more of the following factors.

(ii) Within the spectral region where υ_2 is expected, weak bands due to spin-forbidden transitions to various levels descending from the free-ion term, ^2G, may also appear; the weak υ_2 may be easily confused with any of them. (iii) In octahedral fields of oxygen-coordinating

ligands, the value of the crystal field splitting parameter, Dq, is such that the energy of $^4A_{2g(F)}$ is nearly coincident with that of $^4T_{1g(p)}$. This is expected to cause overlapping of υ_2 and υ_3 leading to masking of the weak υ_2 by the intense broad υ_3 [20]. The electronic spectra data of the Co(II) complex are shown in Fig. 1a. The electronic spectral data reveal four bands at 470, 381, 328 and 246 nm. The band appearing in 246 nm is attributed to $\pi \rightarrow \pi^*$ transition of the benzene ring. Furthermore, the absorption spectra of complex illustrate bands in the 328, 381 nm assigned to the n $\rightarrow \pi^*$ transitions of the azomethine group and to the presence of charge transfer

transition, respectively [21, 22]. Also, band at 470 nm assignable to [$^4T_{1g}$(F) $^4T_{1g}$(P)] transition, characteristic of octahedral geometry [23].

The electronic spectra data of the Cr(III) complex are shown in Fig. 1b. The electronic spectral data reveal three bands at 1123, 311, and 242 nm. The band appearing in 242 nm is attributed to $\pi \rightarrow \pi^*$ transition of the benzene ring. Furthermore, band in the 311 nm is assigned to the $n \rightarrow \pi^*$ transitions of the azomethine group. The electronic spectrum of Cr(III) complex showed band in the range 1123 nm. The spectral band is consistent with that of five-coordinated Cr(III) complex, thus a square-pyramidal geometry may be assigned for this complex [24].

FT-IR spectra of complexes

Figure 2a, b shows the FT-IR spectra of the Co(II) and Cr(III) complexes, respectively. The infrared spectrum provides valuable information regarding the nature of the functional group attached to the metal atom. In the FT-IR spectra of Co(II) complex (Fig. 2a), a strong band at 1624 cm^{-1} is due to the C=N stretching vibration [25]. In

the spectra, no peaks corresponding to unreacted primary amines or carbonyl groups were observed. The appearance of a broad band in the IR spectra of the complex at 3305, 3190 cm^{-1} may be due to υ (–OH) of water [26, 27]. The complex shows band at 1389 cm^{-1} indicating free nitrate group [28]. Bands in the range of 577 and 475 cm^{-1} are due to υ (M–O) and υ (M–N) vibration [29] and the appearance of the vibrations support the involvement of the nitrogen and oxygen atoms of the azomethine and C–O groups complexation with the metal ions under investigation. Reviewing similar research works shows that C=S bond stretching vibration appears around 780 cm^{-1}. Because C=S bond vibration in our complex appeared in 749.14 cm^{-1}, thus we can expect that sulfur atom is coordinated to metal that the other analysis also confirmed it.

In the FT-IR spectra of Cr(III) complex (Fig. 2b), a strong band at 1605 cm^{-1} is due to the C=N stretching vibration [25]. In the spectra, there were no peaks corresponding to unreacted primary amines or carbonyl groups. he appearance of a broad band in the IR spectra of the complex at 3330, 3034 cm^{-1} may be due to υ (–OH) of

Fig. 1 UV–vis spectrum of Co(II) (**a**) and Cr(III) (**b**) complexes (10^{-3} M in ethanol)
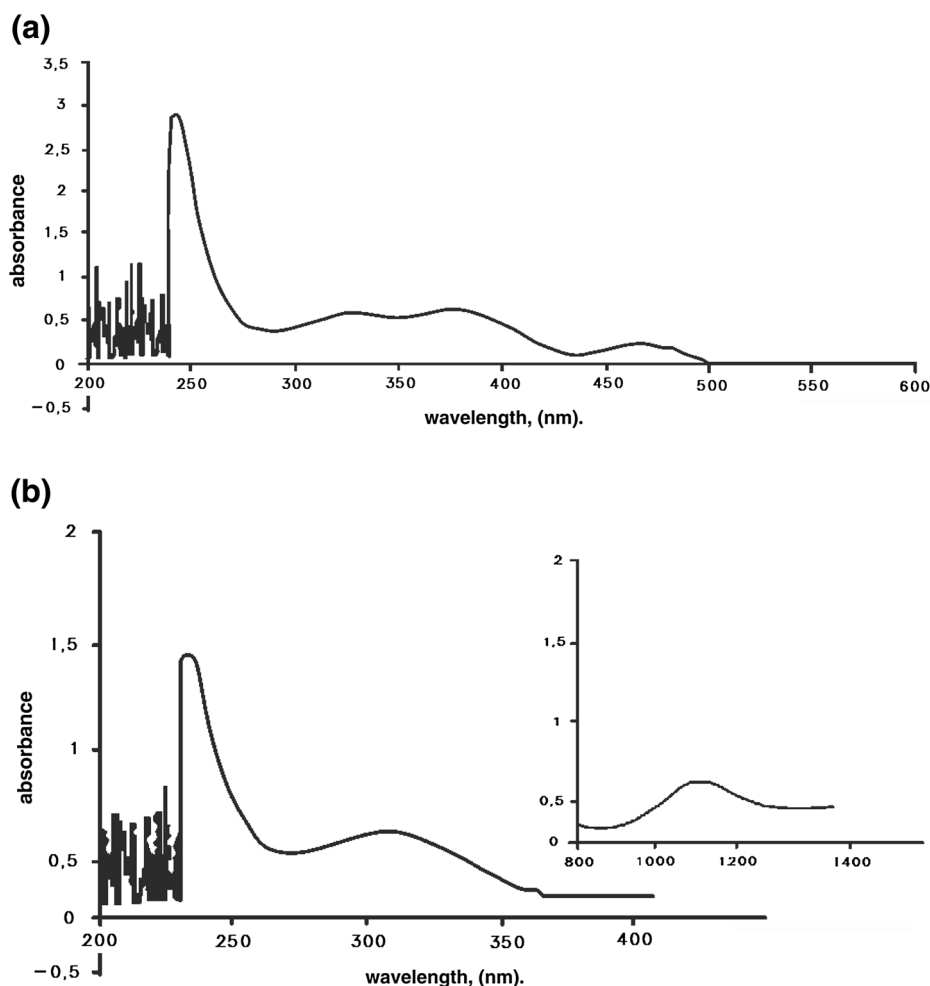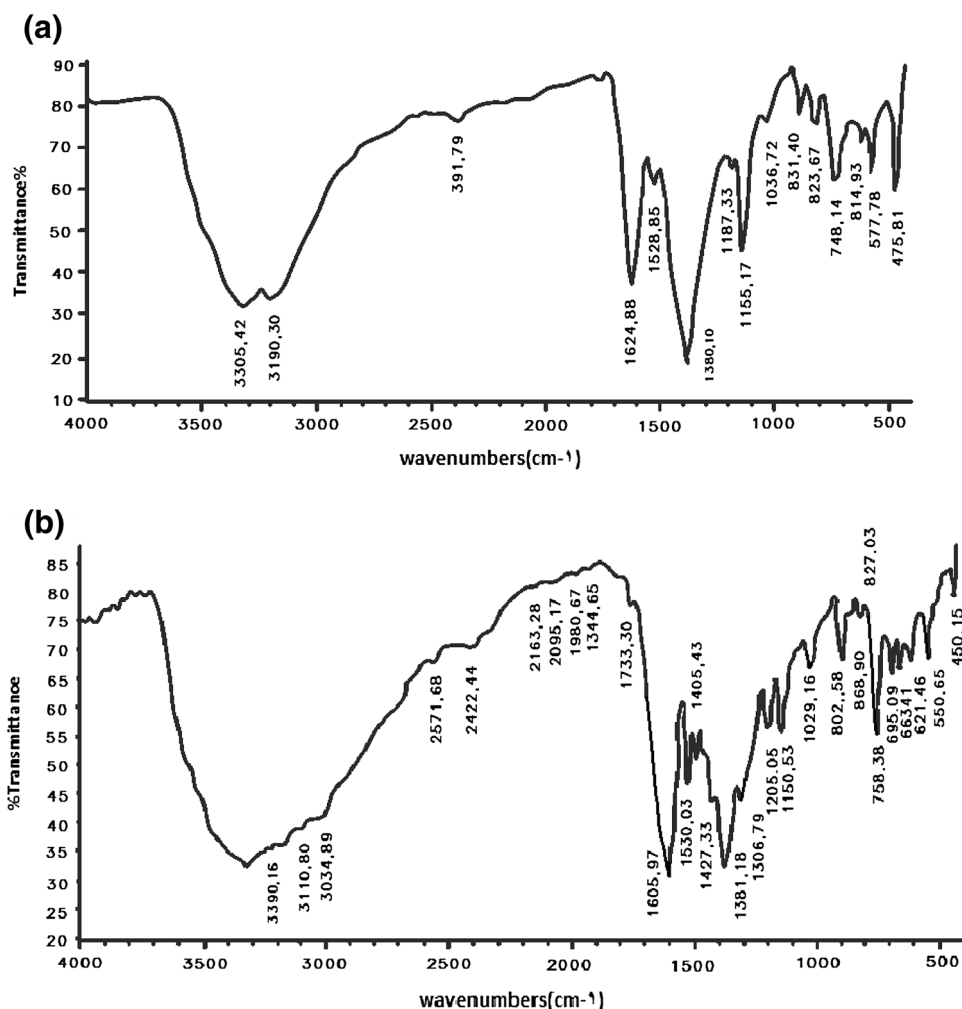
Fig. 2 FT-IR spectra of Co(II) (**a**) and Cr(III) (**b**) complexes

water [26]. The complex shows band at 1381 cm^{-1} indicating free nitrate group [30]. Bands in the range of 550 and 450 cm^{-1} are due to υ(M–O) and υ(M–N) vibration [29] and the appearance of the vibrations confirming the involvement of the nitrogen and oxygen atoms of the azomethine and C–O groups complexation with the metal ions. In this complex as cobalt complex, C=S bond appeared around 758 cm^{-1} confirming coordination of S to metal atom.

FT-IR spectra of metal oxides

In the FT-IR spectrum of Co_3O_4 (Fig. 3a), the broad absorption bands at approximately 3434, 1638 and 1130 cm^{-1} are attributed to the stretching and bending vibrations of the water molecules absorbed by the samples or KBr [31, 32]. The strong bands at 667 cm^{-1} are attributed to the stretching vibration mode of Co–O in which Co is Co^{2+} and is tetrahedrally coordinated. Also, there is a strong band at approximately 574 cm^{-1} on the

spectrum of sample due to Co–O of octahedrally coordinated Co^{3+} [33].

In the FT-IR spectrum of Cr_2O_3 (Fig. 3b) the broad absorption bands at approximately 3436, 1634 and 1131 cm^{-1} are attributed to the stretching and bending vibrations of the water molecules absorbed by the samples or KBr [31, 32]. The strong bands at 633 and 571 cm^{-1} are attributed to the stretching vibration mode of Cr–O [34].

XRD analysis of metal oxides

Crystallinity and crystal phases of the as-synthesized Co_3O_4 and Cr_2O_3 nanoparticles were analyzed. X-ray diffraction patterns of the as-synthesized Co_3O_4 are depicted in Fig. 4a. The patterns show the reflection planes (220), (311), (222), (400), (422), (511), (440), (531), (620), (533) and (622) which indicate the presence of the cubic structure [35]. These diffraction lines provide a clear evidence of the formation of pure Co_3O_4 nanoparticles. In addition, no foreign phases were detected, proving the

Fig. 3 FT-IR spectra of Co_3O_4 (**a**) and Cr_2O_3 (**b**)
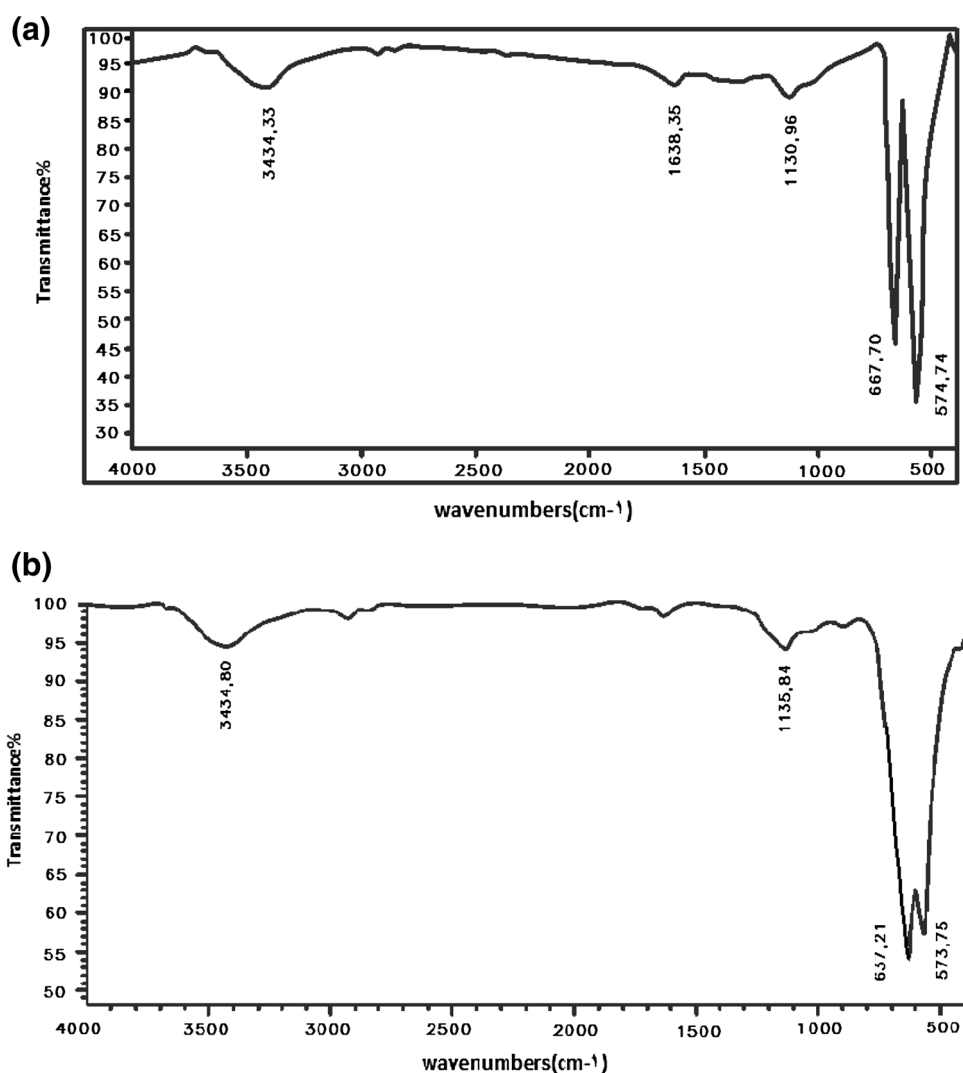
phase purity of the Co_3O_4 products. The average crystallite diameter (*d*) for as-synthesized Co_3O_4 was estimated from the full width at half maximum (FWHM) of the most intense peak (440) by using the Scherrer's formula. The crystallite size is calculated using Debye–Scherrer equation [36–38]:

$$D = 0.9\lambda/\beta \cos\theta,$$

where λ is the X-ray wavelength, β is the line broadening at half the maximum intensity in radians, θ is the Bragg angle. The average particle size determined from XRD peak broadening was found to be close to 32 nm.
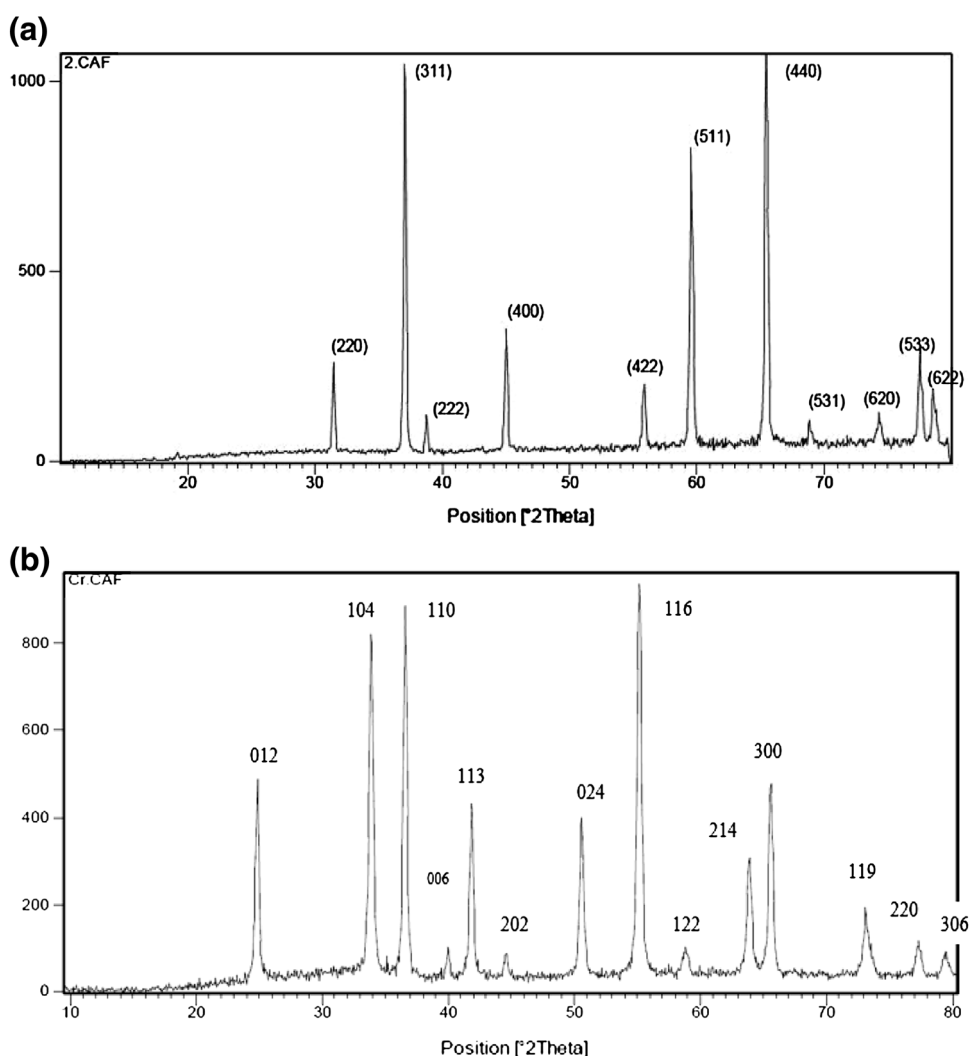
X-ray diffraction patterns of as-synthesized Cr_2O_3 are depicted in Fig. 4b. The patterns show the reflection planes (012), (104), (110), (006), (113), (202), (024), (116), (122), (214), (300), (119), (220) and (306) which indicate the presence of the rhombohedral structure [39]. The crystallite size is calculated by using Debye–Scherrer equation. The

average particle size determined from XRD peak broadening was found to be close to 21 nm.

Scanning electron micrographs (SEM) of metal oxides

Figure 5a shows a scanning electron microscopy image of as-prepared Co_3O_4 nanoparticles. The crystallinity of the Co_3O_4 nanoparticles were well developed and the Co_3O_4 grains had a nearly uniform morphology with an average diameter of approximate 62 nm. Also, Fig. 5b shows a scanning electron microscopy image of as-prepared Cr_2O_3 nanoparticles. The Cr_2O_3 grains had a nearly uniform morphology with an average diameter of approximately 39 nm. In this work, crystalline size is completely different from the particle size because the particle tested by XRD is crystallize size, or named primary particle, which is a single crystal particle but the particle tested by SEM

Fig. 4 XRD pattern of Co$_3$O$_4$ (**a**) and Cr$_2$O$_3$ (**b**)

Applications

Antibacterial activity of complexes in agar medium

The increased rate of mortality due to infectious diseases is directly is concerned to bacteria that exhibit multiple resistance to antibiotics. The lack of effective treatments is the main cause of this problem. The development of new antibacterial agents with novel and more efficient mechanisms of action is definitely an urgent medical need. Thus, the Schiff base complex was tested for in vitro antibacterial activity against *Escherichia coli*, *Staphylococcus aureus*, and *Bacillus subtilis* using the diffusion method. The diffusion method is simple, yet is routinely used in hospital laboratories; it requires commercial disks, the medium used is agar with 2% of glucose and the diameter of the zone of

usually is a particle consisting one or two or even more primary particles.

inhibition is visually read 18 h after incubation at 37 °C. Antibacterial activity was estimated on the basis of the size of the zone of inhibition formed around the paper disks on the seeded agar plates. *Streptomycin* was used as a standard. The results are presented in Table 2. Comparing the biological activity of the metal complex with the standard the following results were obtained: the biological activity of the complexes was close to that of standard. Furthermore, *Bacillus subtilis* and *Escherichia coli* were inhibited to the greatest degree by the Co(II) and Cr(III) complexes; therefore, may be used as antibacterial drug after performing further research works with advanced technology.

Antimicrobial activity of the metal chelates can be explained on the basis of chelation theory which may enhance the biochemical potential of a bioactive species. This is because on chelation, the polarity of the metal ion will be reduced due to the overlap of the ligand orbital and partial sharing of the positive charge of the metal ion with donor groups and possibly electron delocalization over the whole molecule [40–42]. This may enhance the penetration
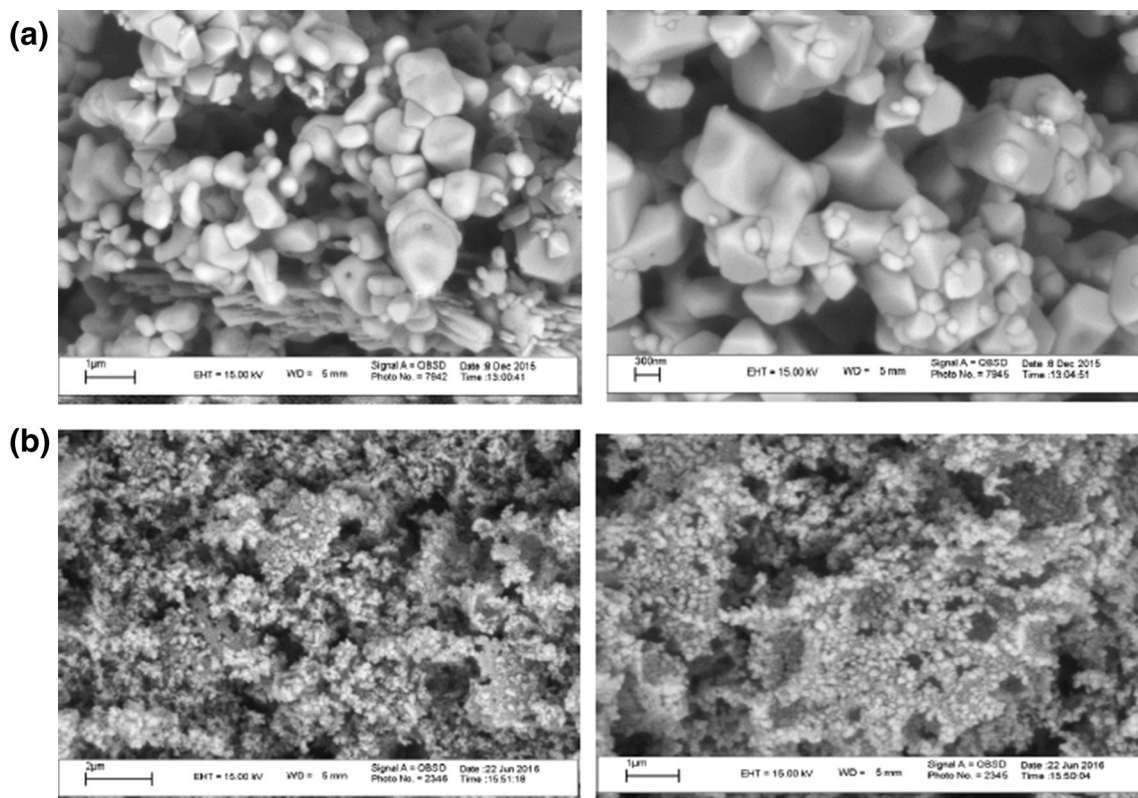
Fig. 5 SEM micrograph of Co_3O_4 (**a**) and Cr_2O_3 (**b**) nanoparticles

Table 2 Antibacterial activity of Co(II) and Cr(III) complexes

Compound (5 mg/L)	Escherichia coli Mean ± RSD	Staphylococcus aureus Mean ± RSD	Bacillus subtilis Mean ± RSD
Co(II) complex (zone of inhibition diameter)	15 mm ± 0.010	13 mm ± 0.034	18 mm ± 0.028
Cr(III) complex (zone of inhibition diameter)	16 mm ± 0.021	10 mm ± 0.029	13 mm ± 0.017
Streptomycin	18 mm ± 0.023	16 mm ± 0.019	20 mm ± 0.022

RSD relative standard deviation

of the complex into the lipid membranes enabling it to block the metal binding sites in the enzymes of microorganisms. These complexes also disturb the respiratory processes of the cell and thus inhibit protein synthesis which restricts further growth of the organism [43]. The mechanism of action of antimicrobial agents can be categorized further based on the structure of the bacteria or the function that is affected by the agents. These include generally the following: (1) inhibition of the cell wall synthesis; (2) inhibition of ribosome function, inhibition of nucleic acid synthesis; (3) inhibition of folate metabolism; (4) inhibition of cell membrane function. Microorganisms were increasingly becoming resistant to ensure their survival against the arsenal of antimicrobial agents to which they were being bombarded. They achieved this through different means, but primarily based on the chemical

structure of the antimicrobial agent and the mechanisms through which the agents acted. The resistance mechanisms therefore depend on which specific pathways are inhibited by the drugs and the alternative ways available for those pathways that the organisms can modify to get a way around in order to survive. Resistance can be described in two ways: (a) intrinsic or natural whereby microorganisms naturally do not posses target sites for the drugs and therefore the drug does not affect them or they naturally have low permeability to those agents because of the differences in the chemical nature of the drug and the microbial membrane structures especially for those that require entry into the microbial cell in order to effect their action or (b) acquired resistance whereby a naturally susceptible microorganism acquires ways of not being affected by the drug [44].

Catalytic oxidation reaction

The reaction was carried out in acetonitrile as solvent, using H_2O_2 as the oxidant and the Co(II) and Cr(III) complexes as the catalyst. In a typical reaction, an aqueous solution of 30% H_2O_2 (15 mmol) and toluene (15 mmol) were mixed in 10 ml of acetonitrile and the reaction mixture was heated at 60 °C. The complex (15 mmol) was added to their action mixture. To this, HNO_3 (10 mmol) was added and their action was considered to be started at this time. During the reaction, the product was analyzed using a gas chromatograph. The effects of various parameters such as concentration of the oxidant and catalyst, temperature and time of the reaction were studied to see their effect on the reaction product. When the Co catalyst is used using optimum reaction conditions (15 mmol H_2O_2, 15 mmol toluene, 60 °C temperature, time 2 h and 15 mmol complex, 10 mmol HNO_3) the toluene conversion to benzyl alcohol and benzaldehyde is maximum. But Cr(III) complex did not show any catalytic activity.

Effect of reaction conditions on toluene oxidation

Effect of time

The appropriate reaction time is the main assurance for the perfect reaction. The catalytic oxidation of toluene, using H_2O_2 as oxidant was studied as a function of time. Table 3 shows that the fit reaction time is 2 h.

Effect of temperature

Table 4 presents the effect of reaction temperature on oxidation of toluene. Five different temperatures (30, 50, 60, 70, 80 °C) were considered, while keeping the other parameters same for the catalytic performance in 10 mL of CH_3CN. Below 60 °C, conversion of toluene was very poor. At the same time above 60 °C, decomposition of H_2O_2 gets accelerated which is not beneficial to toluene oxidation. Thus, 60 °C is the minimum required temperature to supply sufficient energy to reach the energy barrier of toluene transformation.

Table 3 The influence of reaction time

Time (h)	Toluene conversion (%)	Benzyl alcohol (%)	Benzaldehyde (%)
1	9.44	6.15	3.29
2	17.10	15.28	1.82
3	17.25	15.51	1.74
4	17.85	16.23	1.62
5	18.36	16.44	1.92

Reaction temperature 60 °C; catalyst 15 mmol; toluene:H_2O_2 (molar ratio) = 1:1; HNO_3 10 mmol; acetonitrile 10 ml

Table 4 The influence of temperature

Temperature (°C)	Toluene conversion (%)	Benzyl alcohol (%)	Benzaldehyde (%)
30	0	0	0
50	4.13	2.74	1.39
60	12.59	9.28	3.31
70	13.09	10.20	2.89
80	13.20	10.55	2.65

Reaction time 2 h; catalyst 15 mmol; toluene:H_2O_2 (molar ratio) = 1:1; acetonitrile 10 ml; HNO_3 10 mmol

Table 5 The influence of the amount of catalyst

Catalyst (mmol)	Toluene conversion (%)	Benzyl alcohol (%)	Benzaldehyde (%)
5	3.30	2.07	1.23
10	6.38	4.54	1.84
15	16.10	14.48	1.62
20	14.36	12.90	1.46
25	13.01	10.32	2.69

Reaction time 2 h; reaction temperature 60 °C; toluene:H_2O_2 (molar ratio) = 1:1; acetonitrile 10 mL; HNO_3 10 mmol

Effect of amount of catalyst

When the reaction was performed without a catalyst, it did not yield any products. The effect of amount of catalyst on the rate of reaction is shown in Table 5. Five different amounts of the catalyst were used for the fixed amount of toluene (15 mmol) and oxidant (15 mmol) in 10 mL CH_3CN and 10 mmol HNO_3. Results showed that 15 mmol of catalyst can be sufficient enough to give good performance. Lowering the amount of catalyst resulted in the poor conversion.

Effect of H_2O_2 concentration

The amount of H_2O_2 concentration has great influence on reaction rate. Table 6 presents the effect of H_2O_2 concentration on reaction rate. The influence of oxidant on reaction was investigated using five different amounts of aqueous 30% H_2O_2, viz. 15, 20, 25, 30 and 35 mmol for a fixed amount of toluene (15 mmol) and catalyst (15 mmol) in 10 mL CH_3CN and 10 mmol HNO_3. The lowest H_2O_2 concentration results in only ca. 4.7% toluene oxidation. This information suggests that H_2O_2/toluene ratio of 1:1 is ideal for the maximum conversion as well as maximum efficiency. Thus, the larger concentration of oxidant is not an essential condition to maximize toluene conversion.

30% H_2O_2 is a compromise between efficiency and safety. In principle, a higher concentration of H_2O_2 would

Table 6 The influence of H_2O_2 concentration

Hydrogen peroxide (mmol)	Toluene conversion (%)	Benzyl alcohol (%)	Benzaldehyde (%)
15	4.73	4.57	0.16
20	6.49	6.28	0.21
25	14.91	13.89	1.02
30	16.39	14.76	1.63
35	18.01	16.14	1.87

Reaction time 2 h; reaction temperature 60 °C; catalyst 15 mmol; acetonitrile 10 mL; HNO_3 10 mmol

Table 7 The influence of amount of HNO_3

HNO_3 (mmol)	Toluene conversion (%)	Benzyl alcohol (%)	Benzaldehyde (%)
0	0	0	0
5	3.14	2.23	0.91
10	10.36	7.44	2.92
15	11.13	9.89	1.24
20	12.66	10.45	2.21

Reaction time 2 h; reaction temperature 60 °C; catalyst 15 mmol; acetonitrile 10 mL; toluene:H_2O_2 (molar ratio) = 1:1

of course be more efficient, since in heterogeneous catalysis the H_2O diluent can compete with H_2O_2 for active sites on the catalyst surface, and in homogeneous catalysis the rate of the oxidation step involving H_2O_2 is proportional to its concentration. However, in concentrations higher than 30% H_2O_2 is unstable, even at refrigerator temperatures, which is why almost all suppliers limit the concentration to 30%. Stability is not the only reason for this: at higher concentrations H_2O_2 becomes a hazardous substance because of the explosion risks when mixed with organics. Below 30%, the >70% water keeps the temperature increase upon an exothermal reaction with an organic within bounds and so lessens the risk of a thermal runaway.

Effect of amount of HNO_3

It has been evident that nitric acid has a positive role in catalytic reactions. In the presence of nitric acid, decomposition of hydrogen peroxide is slowed down and thus the stability of intermediate is enhanced. The influence of HNO_3 on reaction was investigated using five different amounts of HNO_3. When the oxidation of the substrate is carried out without nitric acid, the reaction does not ensue at all. Results showed that 10 mmol of HNO_3 can be sufficient enough to give good performance (Table 7).

Conclusions

In this paper, Schiff base complexes of the Co^{2+} and Cr^{3+} from salicylaldehyde and thiourea were synthesized and characterized. Then pure Co_3O_4 and Cr_2O_3 nanoparticles with 32 and 21 nm in size for Co(II) and Cr(III), respectively, have been successfully synthesized through the decomposition of Schiff base complex under heating furnace. The solid-state thermal decomposition method is an easy, safe and suitable for high purity production for the preparation of nanoparticles. This method also has potential advantages, including operational simplicity, no need for solvent, low energy consumption and no special

equipment required. The complexes screened for antibacterial activity against some clinically important bacteria such as *Escherichia coli*, *Staphylococcus aureus*, and *Bacillus subtilis*. The biological activity of the Co(II) and Cr(III) complexes showed that these compounds possess antibacterial effect. Catalytic property of the complexes were studied in oxidation of toluene using hydrogen peroxide (H_2O_2) as the oxidant. The Co(II) complex was catalytically active towards toluene, but Cr(III) complex did not show any catalytic activity.

References

1. Mahlooji, N., Behzad, M., Amiri Rudbari, H., Bruno, G., Ghanbari, B.: Unique examples of copper(II)/sodium(I) and nickel(II)/sodium(I) Schiff base complexes with bridging bis-bidentate Salen type ligand: synthesis, crystal structures and antibacterial studies. Inorg. Chim. Acta **445**, 124–128 (2016)
2. Sangamesh, A.P., Chetan, T.P., Bhimashankar, M.H., Shivakumar, S.T., Prema, S.B.: DNA cleavage, antibacterial, antifungal and anthelmintic studies of Co(II), Ni(II) and Cu(II) complexes of coumarin Schiff bases: synthesis and spectral approach. Spectrochim. Acta A **137**, 641–651 (2015)
3. Mokhles, M.A., Ammar, A.L., Hanan, A.M., Samia, A.M., Mamdouh, M.A., Ahmed, A.E.: Synthesis, anticancer activity and molecular docking study of Schiff base complexes containing thiazole moiety. Beni-Suef Univ. J. Appl. Sci. **5**, 85–96 (2016)
4. Jia, L., Xu, J., Zhao, X., Shen, Sh, Zhou, T., Xu, Zh, Zhu, T., Chen, R., Ma, T., Xie, J., Dong, K., Huang, J.: J. Inorg. Biochem. **159**, 107–119 (2016)
5. Adediji, J.F., Olayinka, E.T., Adebayo, M.A., Babatunde, O.: Antimalarial mixed ligand metal complexes: synthesis, physicochemical and biological activities. Int. J. Phys. Sci. **4**, 529–534 (2009)

6. Chang, E.L., Simmers, C., Knight, D.A.: Cobalt complexes as antiviral and antibacterial agents. Pharmaceuticals **3**, 1711–1728 (2010)

7. Abu-Dief, A.M., Mohamed, I.M.A.: A review on versatile applications of transition metal complexes incorporating Schiff bases. J Basic Appl Sci **4**, 119–133 (2015)

8. Abdel-Rahman, L.H., Abu-Dief, A.M., Adam, M.S.S., Hamdan, S.K.: Some new nano-sized mononuclear Cu(II) Schiff base complexes: design, characterization, molecular modeling and catalytic potentials in benzyl alcohol oxidation. Catal. Lett. **146**, 1373–1396 (2016)

9. Menati, S., Amiri Rudbari, H., Khorshidifard, M., Jalilian, F.: A new oxovanadium(IV) complex containing an O,N-bidentate Schiff base ligand: synthesis at ambient temperature, characterization, crystal structure and catalytic performance in selective oxidation of sulfides to sulfones using H_2O_2 under solvent-free conditions. J. Mol. Struct. **1103**, 94–102 (2016)

10. DehnoKhalaji, A., Rahdari, R.: Cobalt(II) macrocycle complexes based synthesis of Co_3O_4 nanoparticles: structural and spectral characterization. Int. J. Bio-Inorg. Hybrid Nanomater. **4**, 209–213 (2015)

11. Abdel-Rahman, L.H., Abu-Dief, A.M., Newair, E.F., Hamdan, S.K.: Some new nano-sized Cr(III), Fe(II), Co(II), and Ni(II) complexes incorporating 2-((E)-(pyridine-2-ylimino)methyl)-napthalen-1-ol ligand: structural characterization, electrochemical, antioxidant, antimicrobial, antiviral assessment and DNA interaction. J. Photochem. Photobiol., B **160**, 18–31 (2016)

12. Abdel-Rahman, L.H., Abu-Dief, A.M., El-Khatib, R.M., Abdel-Fatah, ShM: Some new nano-sized Fe(II), Cd(II) and Zn(II) Schiff base complexes as precursor for metal oxides: sono-chemical synthesis, characterization, DNA interaction, in vitro antimicrobial and anticancer activities. Bioorg. Chem. **69**, 140–152 (2016)

13. Hammam, A.M., EL-Gahami, M.A., Khafagi, Z.A., AL-Salimi, M.S., Ibrahim, S.A.: Synthesis and characterization of some new antimicrobial transition metal complexes with 1,2,4-triazole-3-thione Schiff bases. J. Mater. Environ. Sci. **6**, 1596–1605 (2015)

14. Al-Nahary, T.T.: Synthesis and characterization of metal complexes of Cr(III), Mn(II), Fe(III), Co(II), Ni(II), Cu(II), Ru(III), Rh(III) and Pd(II) with derivatives of 1,3,4-thiadiazole-2,5-dithiol as new ligands. J. Saudi Chem. Soc. **13**, 253–257 (2009)

15. Kumar, M., Singh, A.K.: Synthesis and characterization of complexes of Cobalt(II), Nickel(II) and copper(II) with 2-pyrrolidene-m-nitroaniline and 2-pyrrolidene-p-nitroaniline Schiff bases and their biological activity. Asian J. Chem. **10**, 233–237 (1998)

16. Sharma, A., Shah, M.: Synthesis and characterization of some transition metal complexes derived from bidentate Schiff base ligand. IOSR J. Appl. Chem. **3**, 62–66 (2013)

17. Jha, N.N., Prasad Ray, I.: Magnetic studies of Co(II) and Ni(II) complexes of hydroxamic acid. Asian J. Chem. **12**, 703–706 (2000)

18. Kumar, R., Singh, R.: Chromium(III) complexes with different chromospheres macrocyclic ligands: synthesis and spectroscopic studies. Turk. J. Chem. **30**, 77–87 (2006)

19. Kumar, G., Devi, S.H., Johari, R.: Synthesis and spectral characterization of Schiff base Cr(III), Mn(III), and Fe(III) novel macrocyclic complexes derived from thiocarbohydrazide and dicarbonyl compound. Eur. J. Chem. **9**, 2255–2260 (2012)

20. Askalan, P.: The two-electron transition, $^4T_{1g}(F) \rightarrow {}^4A_{2g}(F)$, in the spectra of octahedral oxygen-coordinated cobalt(II) species. Transit. Met. Chem. **11**, 469–471 (1986)

21. Abdel-Rahman, L.H., Abu-Dief, A.M., Hamdan, S.K., Seleem, A.A.: Nano structure Iron (II) and Copper (II) Schiff base complexes of a NNO-tridentate ligand as new antibiotic agents:

22. Abdel-Rahman, L.H., Abu-Dief, A.M., Ismael, M., Mohamed, M.A.A., Hashem, N.A.: Synthesis, structure elucidation, biological screening, molecular modeling and DNA binding of some Cu(II) chelates incorporating imines derived from amino acids. J. Mol. Struct. **1103**, 232–244 (2016)

23. Ibrahim, O.B., Mohamed, M.A., Refat, M.S.: Nano sized Schiff base complexes with Mn(II), Co(II), Cu(II), Ni(II) and Zn(II) metals: synthesis, spectroscopic and medicinal studies. Can. Chem. Trans. **2**, 108–121 (2014)

24. Kumar, G., Kumar, D., Singh, C.P., Kumar, A., Ranaj, V.B.: Synthesis, physical characterization and antimicrobial activity of trivalent metal Schiff base complexes. Serb. Chem. Soc. **75**, 629–637 (2010)

25. Krishnankutty, K., Ummathur, M.B., Sayudevi, P.: Metal complexes of Schiff bases derived from dicinnamoylmethane and aromatic amines. J. Argent. Chem. Soc. **96**, 13–21 (2008)

26. Wilson, C.Y., Velayudham, S., Manickam, S., Deivanayagam, E.: β-Tolyl alanine derived Schiff base complexes—synthesis characterization and antimicrobial assessment. J. Pharm. Sci. Res. **7**, 25–32 (2015)

27. Sakthilatha, D., Rajavel, R.: Chem. Pharm. Res. **5**, 57–63 (2013)

28. Joseyphus, R.S., Nair, M.S.: Antibacterial and antifungal studies on some Schiff base complexes of Zinc(II). Mycobiology **36**, 93–98 (2008)

29. Deshmukh, P.S., Yaul, A.R., Bhojane, J.N., Aswar, A.S.: Synthesis, characterization and thermogravimetric studies of some metal complexes with N_2O_2 Schiff base ligand, world. Appl. Sci. J. **9**, 1301–1305 (2010)

30. Saghatforoush, L.A., Sanati, S., Marandi, Gh, Hasanzadeh, M.: Synthesis, characterization and catalytic activity of CuO nanostructures using Schiff base copper complexes as a precursor. J. Nanostruct. Chem. **3**, 33–41 (2013)

31. Ahmed, S.R., Kofinas, P.: Magnetic properties and morphology of block copolymer-cobalt oxide nanocomposites. J. Magn. Mater. **288**, 219–223 (2005)

32. Saad El-Zweay, R., MiloudEl-Ajaily, M., FarajBen-Gweirif, S., Maihub, A.: Preparation, characterization and antibacterial activity of some mixed ligand chelates. J. Chem. Soc. Pak. **35**, 67–71 (2013)

33. Zou, D., Xu, C., Lou, H., Wang, L., Ying, T.: Synthesis of Co_3O_4 nanoparticles via an ionic liquid-assisted methodology at room temperature. Mater. Lett. **62**, 1976–1978 (2008)

34. Farzaneh, F., Najafi, M.: Synthesis and characterization of Cr_2O_3 nanoparticles with triethanolamine in water under microwave irradiation. J. Sci. Islam Repub. Iran **22**, 329–333 (2011)

35. Kang, M., Zhou, H.: Facile synthesis and structural characterization of Co_3O_4 nanocubes. AIMS Mater. Sci. **2**, 16–27 (2015)

36. El-Remaily, M.A.A.A.A., Abu-Dief, A.M.: $CuFe_2O_4$ nanoparticles: an efficient heterogeneous magnetically separable catalyst for synthesis of some novel propynyl-1H-imidazoles derivatives. Tetrahedron **71**, 2579–2584 (2015)

37. Abu-Dief, A.M., Nassar, I.F., Elsayed, W.H.: Magnetic $NiFe_2O_4$ nanoparticles: efficient, heterogeneous and reusable catalyst for synthesis of acetylferrocene chalcones and their anti-tumour activity. Appl. Organometal. Chem. **30**, 917–923 (2016)

38. Abu-Dief, A.M., Abdelbaky, M.S.M., Martínez-Blanco, D., Amghouz, Z., García-Granda, S.: Effect of chromium substitution on the structural and magnetic properties of nanocrystalline zinc ferrite. Mater. Chem. Phys. **174**, 164–171 (2016)

39. Tagreed, Al-Saadi, M., Noor, A.H.: Synthesis and structural characterization of Cr_2O_3 nanoparticles prepared by using $Cr(NO_3)_3 \cdot 9H_2O$ and triethanolamine under microwave irradiation. Adv. Phys. Theor. Appl. **44**, 139–148 (2015)

40. Abdel-Rahman, L.H., El-Khatib, R.M., Nassr, L.A.E., Abu-Dief, A.M., Ismail, M., Seleem, A.A.: Metal based pharmacologically active agents: synthesis, structural characterization, molecular modeling, CT-DNA binding studies and in vitro antimicrobial screening of iron(II) bromosalicylidene amino acid chelates. Spectrochim. Acta A **117**, 366–378 (2014)

41. Abu-Dief, A.M., Nassr, L.A.E.: Tailoring, physicochemical characterization, antibacterial and DNA binding mode studies of Cu(II) Schiff bases amino acid bioactive agents incorporating 5-bromo-2-hydroxybenzaldehyde. J. Iran. Chem. Soc. **12**, 943–955 (2015)

42. Abdel-Rahman, L.H., El-Khatib, R.M., Abu-Dief, A.M., Abdel-Fatah, S.M., Sleem, A.A.: Nano structure Iron (II) and Copper (II) Schiff base complexes of a NNO-tridentate ligand as new antibiotic agents: spectral, thermal behaviors and DNA binding ability. Int. J. Nano Chem. **2**, 83–91 (2016)

43. Yiase, S.G., Adejo, S.O., Gbertyo, J.A., Edeh, J.: Synthesis, characterization and antimicrobial studies of salicylic acid complexes of some transition metals. IOSR J. Appl. Chem. **7**, 4–10 (2014)

44. Yousif, E., Majeed, A., Al-Sammarrae, Kh, Salih, N., Salimon, J., Abdullah, B.: Metal complexes of Schiff base: preparation, characterization and antibacterial activity. Arab J. Chem. (2013). doi:10.1016/j.arabjc.2013.06.006